Physics Letters B 736 (2014) 252–260

Contents lists available at ScienceDirect

Physics Letters B

www.elsevier.com/locate/physletb

Top-quark charge asymmetry and polarization in $t\bar{t}W^{\pm}$ production at the LHC

F. Maltoni [a], M.L. Mangano [b], I. Tsinikos [a,*], M. Zaro [c,d]

[a] Centre for Cosmology, Particle Physics and Phenomenology (CP3), Université Catholique de Louvain, Belgium
[b] CERN, PH-TH, Geneva, Switzerland
[c] Sorbonne Universités, UPMC Univ. Paris 06, UMR 7589, LPTHE, F-75005, Paris, France
[d] CNRS, UMR 7589, LPTHE, F-75005, Paris, France

ARTICLE INFO

Article history:
Received 30 June 2014
Accepted 17 July 2014
Available online 23 July 2014
Editor: G.F. Giudice

ABSTRACT

We study the charge asymmetry between the t and $\bar{t}$ quarks at the LHC, when they are produced in association with a W boson. Though sizably reducing the cross section with respect to the inclusive production, requiring a W boson in the final state has two important implications. First, at leading order in QCD, $t\bar{t}W^{\pm}$ production can only occur via $q\bar{q}$ annihilation. As a result, the asymmetry between the t and $\bar{t}$ generated at NLO in QCD is significantly larger than that of inclusive $t\bar{t}$ production, which is dominated by gluon fusion. Second, the top quarks tend to inherit the polarization of the initial-state quarks as induced by the W-boson emission. Hence, the decay products of the top quarks display a sizable asymmetry already at the leading order in QCD. We study the relevant distributions and their uncertainties in the standard model, compare them to those obtained in a simple axigluon model and discuss prospects for measurements at the LHC and beyond.

1. Introduction

The charge asymmetry in $t\bar{t}$ production at pp colliders is defined by the quantity:

$$A_c^t = \frac{N(\Delta_\eta^t > 0) - N(\Delta_\eta^t < 0)}{N(\Delta_\eta^t > 0) + N(\Delta_\eta^t < 0)}, \tag{1}$$

where $\Delta_\eta^t = |\eta_t| - |\eta_{\bar{t}}|$. Quantum chromodynamics (QCD) predicts that radiative corrections to the leading-order (LO) $t\bar{t}$ production process induce a non-vanishing A_c^t, implying that top quarks are produced with a rapidity distribution wider than anti-top quarks. At next-to-leading order (NLO), this effect was first calculated in Refs. [1,2]. The interest in this asymmetry stems from measurements of the corresponding forward–backward asymmetry (A_{FB}) performed in $p\bar{p}$ collisions at the Tevatron by the CDF and DØ Collaborations [3–7]. These measurements point to a departure from the SM predictions [1,2,8–13], giving rise to a large literature of possible interpretations based on physics beyond the Standard Model (BSM) (for a recent review, see [14]).

Unfortunately, the charge asymmetry predicted by the Standard Model (SM) at the LHC is much smaller than A_{FB} at the Tevatron. The main reason is that both A_{FB} and A_c are induced only by the fraction of $t\bar{t}$ final states generated by $q\bar{q}$ collisions, which at the LHC represent only $\sim 15\%$ of the total rate, compared to $\sim 85\%$ at the Tevatron. The smallness of the effect makes it difficult at the LHC to reach the sensitivity required to measure A_c^t, and to probe the possible existence of BSM contributions, unless the BSM departures from the SM prediction were rather large.

The measurements of top charge asymmetry performed so far by the ATLAS and CMS Collaborations [15–19], have reached uncertainties at the level of $\delta A_c^t \sim 0.01$, which is of the order of the SM value of A_c^t. For example, in their latest publications relative to data taken at $\sqrt{s} = 7$ TeV, ATLAS [15] and CMS [19] report the following results[1]:

$$\text{ATLAS:} \quad A_{c,y}^t = 0.006 \pm 0.010_{\text{stat+syst}}, \tag{2}$$

$$\text{CMS:} \quad A_{c,y}^t = -0.010 \pm 0.017_{\text{stat}} \pm 0.008_{\text{syst}}, \tag{3}$$

$$\text{CMS:} \quad A_c^\ell = 0.009 \pm 0.010_{\text{stat}} \pm 0.006_{\text{syst}}. \tag{4}$$

[1] The LHC measurements are reported in terms of rapidity differences $\Delta_y^t = |y_t| - |y_{\bar{t}}|$, and we shall refer to these asymmetries as $A_{c,y}$. Charge asymmetries based on rapidity differ by about 10–20% from those based on pseudorapidity, but have otherwise the same features. Here the leptonic asymmetries A_c^ℓ are defined by replacing in Eq. (1) Δ_η^t with $\Delta_\eta^\ell = |\eta_{\ell^+}| - |\eta_{\ell^-}|$. In the following we shall also consider A_c^b, defined by $\Delta_\eta^b = |\eta_b| - |\eta_{\bar{b}}|$.

* Corresponding author.

http://dx.doi.org/10.1016/j.physletb.2014.07.033

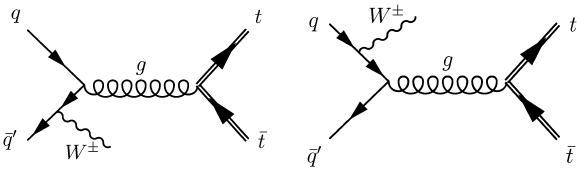

Fig. 1. Feynman diagrams for the $t\bar{t}W^{\pm}$ production at leading order in QCD.

A combination of the ATLAS and CMS results has also been performed by the Top LHC Working Group [20]

$$A^t_{c,y} = 0.005 \pm 0.007 \pm 0.006. \tag{5}$$

The SM result used as a comparison in the experimental papers, including both QCD and electroweak (EW) radiative corrections at the one-loop level, is obtained from Ref. [13]:

$$A^t_{c,y}(7\text{ TeV}) = 0.0123 \pm 0.0005, \tag{6}$$

$$A^{\ell}_{c}(7\text{ TeV}) = 0.0070 \pm 0.0003. \tag{7}$$

These values[2] result from using the LO total cross sections in the denominator of Eq. (1). This is justified by the fact that, at the one-loop level, the asymmetry is an LO effect. Using the NLO total cross section, which is $\sim 50\%$ larger than the LO one, the calculated asymmetries would be reduced to $\sim 2/3$ of the above values. We believe that, in absence of a complete NLO calculation of A^t_c, the difference between the use of LO and NLO cross sections in the denominator of Eq. (1) should be included in the estimate of the overall theoretical uncertainty. Should the true SM value of A^t_c end up being closer to the smaller values obtained using the NLO cross sections (e.g. $A^t_c \sim 0.004$ at $\sqrt{s} = 14$ TeV), a robust and accurate measurement will be a hard experimental challenge.

Alternative observables are known to enhance the size of the asymmetry. For example, Ref. [13] estimates that the asymmetry can increase by a factor of 2–3 placing proper cuts on the invariant mass of the $t\bar{t}$ system. The smaller rates due to the extra cuts will be compensated by the much larger statistics to become available at 13–14 TeV. But the theoretical systematics will, by and large, remain correlated with those of the predictions for the underlying fully inclusive A^t_c.

In this work, we therefore consider an alternative production mechanism for top quark pairs, which can provide a complementary handle for the determination of the SM charge asymmetry, as well as an independent probe of possible BSM sources of a deviation from the SM result. The mechanism we propose is the production of a $t\bar{t}$ pair in association with a W boson (Fig. 1). This production process is indeed quite peculiar. At the LO in QCD it can only occur via a $q\bar{q}$ annihilation, and no contribution from gluons in the initial states is possible. This is at variance with respect to $t\bar{t}Z$ or $t\bar{t}\gamma$, where the vector boson can also couple to the top quark in the subprocess $gg \to t\bar{t}$. As it can be seen from Fig. 1, $t\bar{t}W^{\pm}$ can be simply thought of as the standard $q\bar{q} \to t\bar{t}$ LO diagram, with the $W^{\pm}$ emitted from the initial state. At the NLO, the qg channels can open up, yet the gluon–gluon fusion production is not accessible until NNLO. As in $q\bar{q} \to t\bar{t}$ the top and the anti-top are produced symmetrically at LO and an asymmetry arises only starting at NLO due to interference effects. As we will show in the following, the absence of the symmetric gluon–gluon channel makes the resulting asymmetry significantly larger than in $t\bar{t}$ production.

[2] The asymmetries for higher beam energies are determined in Ref. [13] to be $A^t_{c,y}(8\text{ TeV}) = 0.0111 \pm 0.0004$ and $A^t_{c,y}(14\text{ TeV}) = 0.0067 \pm 0.0004$.

Table 1
Total cross sections and the asymmetry A^t_c for $pp \to t\bar{t}$, calculated at NLO fixed order, LO + PS, and NLO + PS at 8 TeV. The quoted uncertainties are estimated with scale variations, except for LO + PS A^t_c where they are from MC statistics. For the NLO (+ PS) A^t_c MC uncertainties are less than 0.1 (absolute value in %).

$t\bar{t}$	LO + PS	NLO	NLO + PS
σ (pb)	$128.8^{+35\%}_{-24\%}$	$198^{+15\%}_{-14\%}$	
A^t_c (%)	0.07 ± 0.03	$0.61^{+0.10}_{-0.08}$	$0.72^{+0.14}_{-0.09}$

The second key feature of $t\bar{t}W^{\pm}$ is that the emission of the W boson from the initial state acts as a polarizer for quark and anti-quarks, effectively leading to the production of polarized top and anti-top quarks. In other words, the W-boson emission makes the production of a $t\bar{t}$ pair similar to that in polarized e^+e^- collisions [21–24]. As a result, the decay products of the top and anti-top display very asymmetrical distributions in rapidity already at the leading order. We shall call this the EW component of the asymmetry. In new physics scenarios, the emission of a W boson might also act as a discriminator of the chirality structure of new interactions, such as that of an axigluon with light quarks, as already advocated in different studies [25–27].

Results at the NLO and NLO + PS for the processes $t\bar{t}V$ ($V = W^{\pm}, Z$) have appeared in the literature [28–34] yet no special attention has been given to asymmetries, whether EW or QCD. The effect on the asymmetry due to the emission of a photon has been recently studied in Ref. [35]. Measurements of total rates are also becoming available from the LHC experiments [36].

The plan of this article is as follows. In Section 2 we present the predictions, at NLO in QCD (with and without including parton shower and hadronization effects) for A^t_c in both $t\bar{t}$ and $t\bar{t}W^{\pm}$ production, and, in the latter case, for the asymmetries of the decay products A^b_c and A^{ℓ}_c. In Section 3, we compare the SM predictions to a simple benchmark model featuring an axigluon compatible with the Tevatron A_{FB} measurements, along the lines of what done in Ref. [37], to illustrate the peculiar discriminating power of $t\bar{t}W^{\pm}$. In the final section we discuss the prospects at present and future colliders and present our conclusions. In Appendix A, we review the main features of the polarized $q\bar{q}$ annihilation into $t\bar{t}$, highlighting the close similarity of angular distributions with those predicted in $q\bar{q} \to t\bar{t}W^{\pm}$.

2. $t\bar{t}$ and $t\bar{t}W^{\pm}$ at NLO and NLO + PS

In order to study the top charge asymmetry at NLO for both $t\bar{t}$ and $t\bar{t}W^{\pm}$, we employ MadGraph5_aMC@NLO, a framework [38] which allows to automatically generate the code needed to compute the cross section and any other observable for these (and any other SM) processes at LO, NLO and NLO + PS. We present results computed using the MSTW 2008 (N)LO PDF set [39] with five massless flavors. The pole mass of the top quark is set to 173 GeV and the W-boson mass to 80.41 GeV. The renormalization and factorization scales are kept fixed and set to $\mu_f = \mu_r = 2m_t$, and the corresponding uncertainty is obtained by varying the two scales independently in the interval $[m_t, 4m_t]$. PDF uncertainties are calculated following the Hessian recipe given in Ref. [39]. As we have found that they are negligible in the case of A^t_c (at the level of 0.01 percent), we do not display them in the tables.

We first show in Table 1 the cross section and asymmetry A^t_c for $pp \to t\bar{t}$, computed at the LHC with a center-of-mass energy $\sqrt{s} = 8$ TeV. At the LO there is no top-quark charge asymmetry, while including the parton shower generates a small asymmetry, as shown in Ref. [40]. At NLO a small asymmetry appears (less than 1%) both in the fixed order as well as in the NLO + PS computation, the latter being slightly larger [40]. Not surprisingly,

Table 2
Total cross sections (LO and NLO) and the asymmetry A_c^t (NLO and NLO + PS) for $pp \to t\bar{t}W^{\pm}$ at 8 TeV. The quoted uncertainties are estimated with scale variations. For the asymmetries MC uncertainties are less than 0.1 (absolute value in %).

	Order	$t\bar{t}W^{\pm}$	$t\bar{t}W^{+}$	$t\bar{t}W^{-}$
σ (fb)	LO	$140.5^{+27\%}_{-20\%}$	$98.3^{+27\%}_{-20\%}$	$42.2^{+27\%}_{-20\%}$
	NLO	$210^{+11\%}_{-11\%}$	$146^{+11\%}_{-11\%}$	$63.6^{+11\%}_{-11\%}$
A_c^t (%)	NLO	$2.49^{+0.75}_{-0.34}$	$2.73^{+0.74}_{-0.42}$	$2.03^{+0.81}_{-0.19}$
	NLO + PS	$2.37^{+0.56}_{-0.38}$	$2.51^{+0.62}_{-0.42}$	$1.90^{+0.51}_{-0.35}$

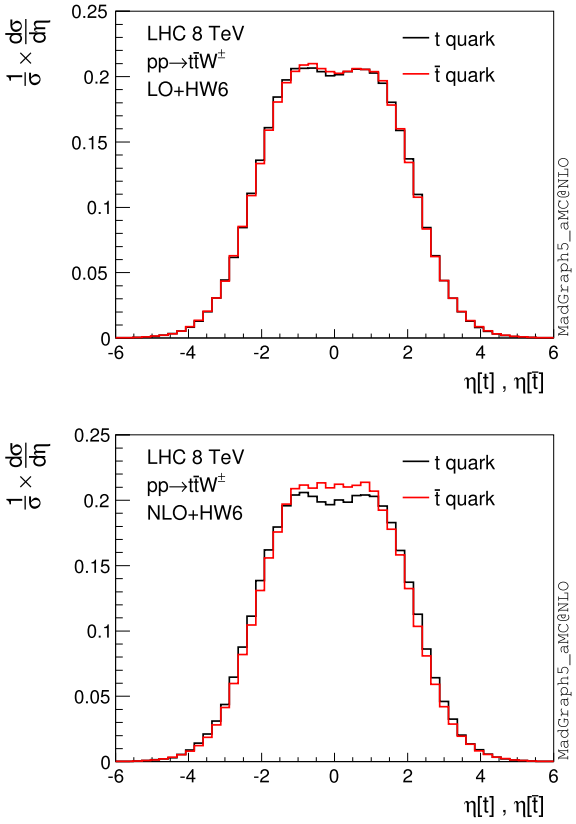

Fig. 2. Comparison of the η distributions of the $t, \bar{t}$ quarks at the (N)LO + PS level for the $pp \to t\bar{t}W^{\pm}$ channel.

a rather strong scale dependence affects the asymmetry predictions, these being *de facto* LO quantities. Here and below, we shall always use the NLO cross sections in the denominators of the asymmetries, leading to a possible underestimate of the real asymmetry. As stated above, we believe that the difference between using LO and NLO cross sections in the denominators should anyway be considered as an additional component of the theoretical systematics (though, this is not accounted for in the scale uncertainties quoted throughout the paper).

We now turn to the corresponding results for $t\bar{t}W^{\pm}$, which are shown in Table 2. As in the previous case, A_c^t vanishes at the LO, but at NLO we obtain $A_c^t \approx 2$–3%, a considerably larger value than in the $t\bar{t}$ inclusive production. The effect of the asymmetry can be visualized by superimposing the pseudorapidity of the t and $\bar{t}$ quarks, as shown in Fig. 2. At LO the two distributions are not distinguishable, while at NLO the asymmetry is manifest: the anti-top quark tends to be more central, whereas the top quark has a broader spectrum, with a dip at $\eta = 0$. Again, the scale dependence of the asymmetry is quite large, consistently with the fact that NLO corrections only provide its LO contribution. The scale dependence

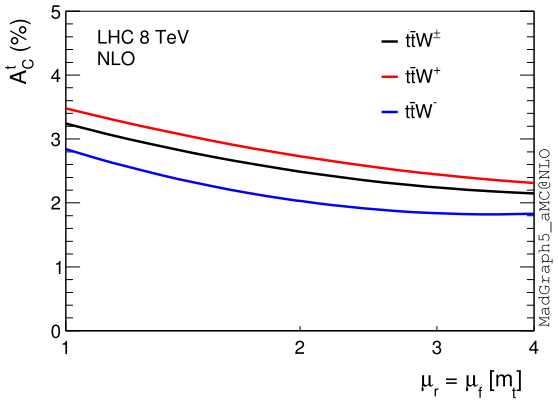

Fig. 3. A_c^t asymmetry at fixed NLO.

of the asymmetry is shown in Fig. 3, varying the renormalization and factorization scales together.

It is also worth to briefly comment on the fact that the asymmetry is larger for $t\bar{t}W^{+}$ than for $t\bar{t}W^{-}$. This can be understood using an argument based on PDF's: the main subprocesses in these two channels are $u\bar{d} \to t\bar{t}W^{+}$ and $d\bar{u} \to t\bar{t}W^{-}$, respectively. The longitudinal momenta of the initial partons are on average $p_u > p_d > p_{\bar{u}} \approx p_{\bar{d}}$. In both cases the momentum of the $t(\bar{t})$ quark is connected to the momentum of the $q(\bar{q})$. The large longitudinal momentum transferred to the t quark from the initial u quark ($t\bar{t}W^{+}$) increases the corresponding $|\eta_t|$ value. As a result the asymmetry A_c^t is enhanced compared to the $t\bar{t}W^{-}$ final state.

As a next step, we consider the case of an NLO + PS simulation, obtained by matching the NLO calculation to HERWIG6 [41] via the MC@NLO method [42]. We show the corresponding results in the third line of Table 2. The asymmetry at LO + PS (not shown in the table) remains zero within uncertainties. At the NLO + PS level a small decrease compared to fixed NLO is found.

Finally, we analyze the results obtained including the decays of the top quarks and the W-boson. In order to keep spin correlations intact for the final lepton and b, $\bar{b}$ distributions, MADSPIN [43] is employed. In so doing parton-level events are decayed using the full tree-level matrix element $2 \to 8$ for the Born-like contributions and $2 \to 9$ for those involving extra radiation, before they are passed to HERWIG6.

At this exploratory stage, we use the MC truth in order to correctly identify leptons and b-jets coming from the top and anti-top quark decays, without considering issues related with the top quark reconstruction. Furthermore we ask that the leptons coming from top (anti) quark decays are positrons (electrons), while the extra W bosons decay into muons, requiring the following decay chains:

- $t \to bW^{+} \to be^{+}\nu_e$,
- $\bar{t} \to \bar{b}W^{-} \to \bar{b}e^{-}\bar{\nu}_e$,
- $W^{-} \to \mu^{-}\bar{\nu}_{\mu}$,
- $W^{+} \to \mu^{+}\nu_{\mu}$.

We present the asymmetries A_c^b and A_c^{ℓ} in Table 3. The former is computed by reconstructing the b-jets in the event which come from the top and anti-top quarks. We cluster hadrons into jets using the k_T algorithm as implemented in FASTJET [44], with $R = 0.7$, $p_T > 20$ GeV and $|\eta| < 4.5$. Smaller values of the R parameter have been checked not to alter significantly the results. For the computation of A_c^b, events that do not feature two b-jets coming from the top quarks have been discarded.

Two observations on the effects of NLO corrections can be made. The first is that for both A_c^{ℓ} and A_c^b NLO corrections tend to shift the EW asymmetries towards positive values, an effect which

Table 3
Asymmetries $A_c^{b,\ell}$, calculated at LO + PS and NLO + PS level, for $pp \to t\bar{t}W^{\pm}$ at 8 TeV. The quoted uncertainties are estimated with scale variations. Figures in the table have around 0.1% of statistical uncertainty.

	Order	$t\bar{t}W^{\pm}$	$t\bar{t}W^{+}$	$t\bar{t}W^{-}$
A_c^b (%)	LO + PS	$7.46^{+0.04}_{-0.05}$	$8.04^{+0.05}_{-0.06}$	$5.67^{+0.01}_{-0.01}$
	NLO + PS	$8.50^{+0.15}_{-0.10}$	$9.39^{+0.15}_{-0.10}$	$6.85^{+0.14}_{-0.11}$
A_c^ℓ (%)	LO + PS	$-17.10^{-0.09}_{+0.11}$	$-18.65^{-0.12}_{+0.14}$	$-13.53^{-0.01}_{+0.03}$
	NLO + PS	$-14.83^{-0.65}_{+0.95}$	$-16.23^{-0.72}_{+1.04}$	$-11.97^{-0.50}_{+0.75}$

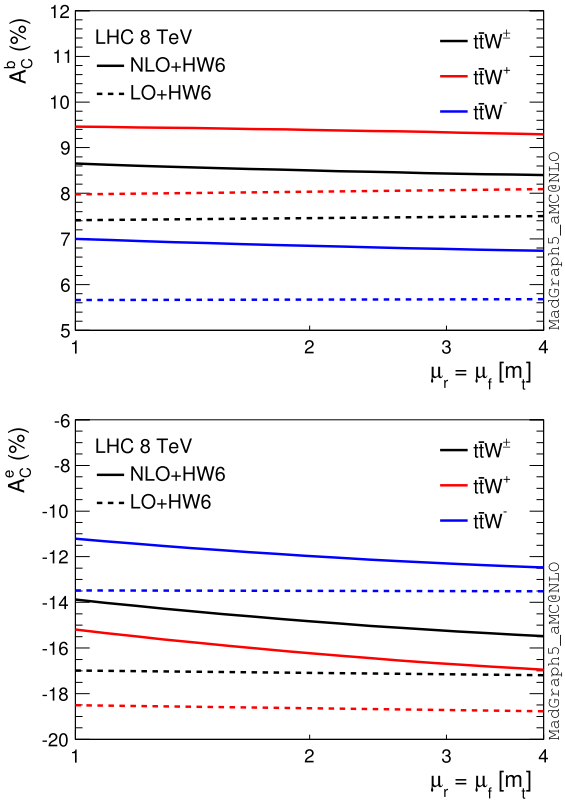

Fig. 4. Comparison of the A_c^b, A_c^ℓ asymmetries between LO + PS and NLO + PS. For all the three channels the dashed line (solid) is the LO + PS (NLO + PS).

is consistent with A_c^t being positive at the NLO. It is not possible to exactly factorize the EW and QCD components of A_c^ℓ and A_c^b, but one can estimate the intrinsic QCD part by suppressing the polarization correlations in the decays, thus removing the EW contribution. In this case, we obtain $A_c^\ell = 1.79$ and $A_c^b = 2.0$, comparable to $A_c^t = 2.37$.

The second observation is that the scale dependence of these asymmetries is very small at the LO, while it becomes larger at the NLO, as it can be seen in Fig. 4. This is due to the fact that the asymmetry at LO is purely EW in origin, and it therefore rather stable against scale variations, while the asymmetry at NLO includes the QCD effects, and is directly affected by the scale dependence.

3. BSM: the axigluon model

The Tevatron experiments (CDF, DØ) have measured the forward–backward asymmetry, which is defined in a similar way to the peripheral-central asymmetry used for the LHC, *i.e.*,

$$A_{t\bar{t}} = \frac{N(\Delta_\eta^{t\bar{t}} > 0) - N(\Delta_\eta^{t\bar{t}} < 0)}{N(\Delta_\eta^{t\bar{t}} > 0) + N(\Delta_\eta^{t\bar{t}} < 0)}, \quad \Delta_\eta^{t\bar{t}} = \eta_t - \eta_{\bar{t}}. \tag{8}$$

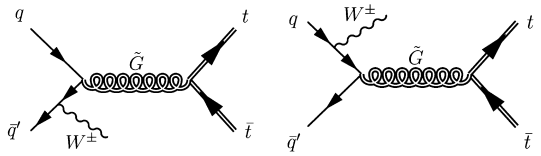

Fig. 5. Leading order Feynman diagrams for the $pp \to t\bar{t}W^{\pm}$ process via an s-channel axigluon.

The central values of the measurements from the two collaborations [3,6] are larger than the SM [13,11],

CDF: $A_{t\bar{t}} = 16.4 \pm 4.7\%$, DØ: $A_{t\bar{t}} = 19.6 \pm 6.5\%$,

SM: $A_{t\bar{t}} = 8.8 \pm 0.6\%$.

A simple toy model that is often used to describe the enhancement of the forward–backward asymmetry at the Tevatron features a massive color octet vector boson (axigluon, $\tilde{G}$) [45,46] that in general can couple in a different way to light and heavy quarks. The enhancement is a result of interference between the LO SM (Fig. 1) and the BSM amplitude (Fig. 5). Studies have already been performed in order to calculate the forward–backward (Tevatron) as well as the central-peripheral (LHC) asymmetry predicted by this model for the $t\bar{t}$ channel [37,47].

We now study how an axigluon would manifest itself in a $t\bar{t}W^{\pm}$ final state. To this aim, and to keep this part as simple as possible, we restrict our BSM predictions to the LO. In general, the axigluon couplings to the quarks are related to the strong coupling g_s and can either be universal (same couplings between light and top quarks) or non-universal. The parameter space of the model provides the freedom to choose a light or a heavy axigluon. The term in the Lagrangian that describes the coupling of the axigluon to quarks is

$$\mathcal{L} = \sum_i \tilde{G}^{\mu,a}\big[g_L^i \bar{q}_i T^a \gamma_\mu (1-\gamma^5) q_i + g_R^i \bar{q}_i T^a \gamma_\mu (1+\gamma^5) q_i\big], \quad i = u, d, t. \tag{9}$$

By choosing $g_L^i = 0$, $g_R^i \neq 0$, a pure right-handed coupling is possible. However, as argued in Appendix A, in $t\bar{t}W^{\pm}$ the initial quark line can only be left-handed, leading to vanishing amplitudes for right-handed axigluons. This brings the first very important difference with respect to $t\bar{t}$ production whose total rates are not sensitive to the relative amount L and R chiralities of the couplings of the axigluon. This is just an example of a more general point: comparing asymmetries in $t\bar{t}$ and $t\bar{t}W^{\pm}$ (and also other associated productions such as with Z and γ) could provide further key information on the new physics interactions. To illustrate this in the case of the axigluon in a quantitative way, we consider four scenarios, two (left, axial) for a light axigluon and two for a heavy one. The light axigluon is chosen to have universal couplings and a fixed width $\Gamma_{\tilde{G}} = 50$ GeV, while the heavy axigluon is chosen to have non-universal couplings and of opposite sign between the light and top quark couplings. The model used for the light axigluon is available from the FeynRules model database [48,49] though it has been slightly modified in order to include non-universal couplings for the heavy axigluon. For the light axigluon ($m_{\tilde{G}} = 200$ GeV, $\Gamma_{\tilde{G}} = 50$ GeV) the scenarios considered are:

Left-handed (I):

$$g_L^u = g_L^d = 0.5 g_s, \qquad g_R^u = g_R^d = 0,$$

Axial (II):

$$g_L^u = g_L^d = -0.4 g_s, \qquad g_R^u = g_R^d = 0.4 g_s.$$

Table 4
Total asymmetries A_c^i, calculated for $pp \to t\bar{t}W^{\pm}$ at 8 TeV. Figures in the table have around 0.1 (%) of statistical uncertainty.

NLO + BSM ($\mu_f = \mu_r = 2m_t$)	A_c^t (%)	A_c^b (%)	A_c^ℓ (%)
$m_{\tilde{G}} = 200$ GeV, left-handed	5.23	10.67	−13.42
$m_{\tilde{G}} = 200$ GeV, axial	6.69	11.55	−11.96
$m_{\tilde{G}} = 2000$ GeV, left-handed	8.76	13.50	−9.02
$m_{\tilde{G}} = 2000$ GeV, axial	7.63	12.55	−10.25

Table 5
Total asymmetries A_c^i, calculated for $pp \to t\bar{t}W^{\pm}$ at 13 TeV. Figures in the table have around 0.1 (%) of statistical uncertainty.

NLO + BSM ($\mu_f = \mu_r = 2m_t$)	A_c^t (%)	A_c^b (%)	A_c^ℓ (%)
$m_{\tilde{G}} = 200$ GeV, left-handed	4.73	9.91	−11.93
$m_{\tilde{G}} = 200$ GeV, axial	6.28	10.61	−10.37
$m_{\tilde{G}} = 2000$ GeV, left-handed	11.54	15.53	−3.45
$m_{\tilde{G}} = 2000$ GeV, axial	7.35	11.13	−7.46

For the heavy axigluon ($m_{\tilde{G}} = 2$ TeV) the decay width is calculated internally [50] considering the decays of the axigluon to quarks (and using $\alpha_S(m_{\tilde{G}})$) the scenarios are:

Left-handed (III):

$$g_L^u = g_L^d = -0.8 g_s, \qquad g_R^u = g_R^d = 0,$$
$$g_L^t = 6 g_s, \qquad g_R^t = 0, \qquad \Gamma_{\tilde{G}} = 1123 \text{ GeV}.$$

Axial (IV):

$$g_L^u = g_L^d = 0.6 g_s, \qquad g_R^u = -0.6 g_s, \qquad g_R^d = 0,$$
$$g_L^t = -4 g_s, \qquad g_R^t = 4 g_s, \qquad \Gamma_{\tilde{G}} = 742 \text{ GeV}.$$

In order to calculate the asymmetries at the best of our knowledge we combine additively the NLO prediction for the SM to the BSM one at LO, *i.e.*,

$$\sigma_{\text{tot}} \equiv \sigma_{\text{NLO}}^{\text{SM}} + \sigma_{\text{LO}}^{\text{BSM}},$$

where

$$\sigma_{\text{LO}}^{\text{BSM}} = |A_{\tilde{G}} + A_{\text{SM}}|^2 - |A_{\text{SM}}|^2,$$

i.e., the contribution of the diagram featuring the axigluon exchange squared as well as the interference with the SM amplitude. For consistency, we employ NLO PDF's in both SM and BSM terms.

The total asymmetry reads

$$A_c = \frac{\sigma_{NLO}^{\text{SM}}}{\sigma_{\text{tot}}} A_c^{\text{SM}} + \frac{\sigma_{\text{LO}}^{\text{BSM}}}{\sigma_{\text{tot}}} A_c^{\text{BSM}}. \tag{10}$$

All results include showering and hadronization. The effect of the axigluon BSM is calculated using Eq. (10) and the results are presented in Tables 4 and 5 (at 8 and 13 TeV respectively), with the scales $\mu_f = \mu_r = 2m_t$. We include the uncertainties due to scale variation ($\mu_f = \mu_r = m_t, 2m_t, 4m_t$) separately for the three A_c^i asymmetries in Fig. 6 (Fig. 7) for $\sqrt{s} = 8$ TeV ($\sqrt{s} = 13$ TeV).

To compare with the sensitivity of the standard charge asymmetry in $t\bar{t}$ final states, we show the results for 13 TeV in Fig. 8. These plots, compared to those in Fig. 7, show that the relative impact of BSM modifications is larger for the $t\bar{t}W^{\pm}$ asymmetries than for the $t\bar{t}$ ones. The reason is that any asymmetry in the $t\bar{t}$ final state, whether induced by QCD effects or by BSM physics, is largely washed out by the symmetric contribution due to the gg initial state. Of course the ultimate reach of measurements in the $t\bar{t}W^{\pm}$ is challenged by the reduced statistics; we shall show in the next section that the high luminosities expected in future runs of the LHC are sufficient to precisely measure the SM asymmetries, and to expose possible BSM contributions.

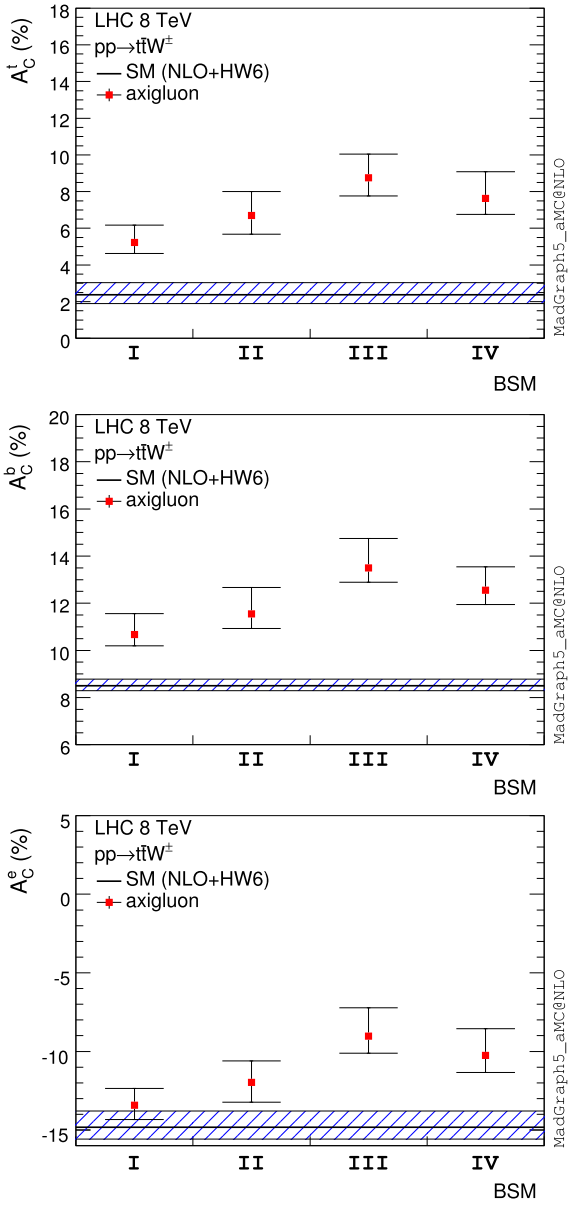

Fig. 6. Comparison between asymmetries predicted in the axigluon (NLO + BSM, I–IV) scenarios and the NLO SM prediction at 8 TeV, including scale uncertainties.

4. Outlook and conclusions

In the previous sections we have argued that the polarization and asymmetry effects in $t\bar{t}W^{\pm}$ production are large enough to offer a useful handle to constrain new physics effects. The question, however, is whether such effects will be measurable given the expected cross sections and luminosities at present and future colliders. To this aim, we have calculated the cross section for the $t\bar{t}W^{\pm}$ process (Table 6) at various pp collider energies, as well as the corresponding asymmetries A_c^i, $i = t, b, e$. For comparison, we also show the results for inclusive $t\bar{t}$ production.

To start with, we observe the steady reduction with beam energy of the leptonic and b asymmetries. This is due to the growing role of the qg initial-state channel (shown in Table 7), which dilutes the EW component of the asymmetry of the decay products.

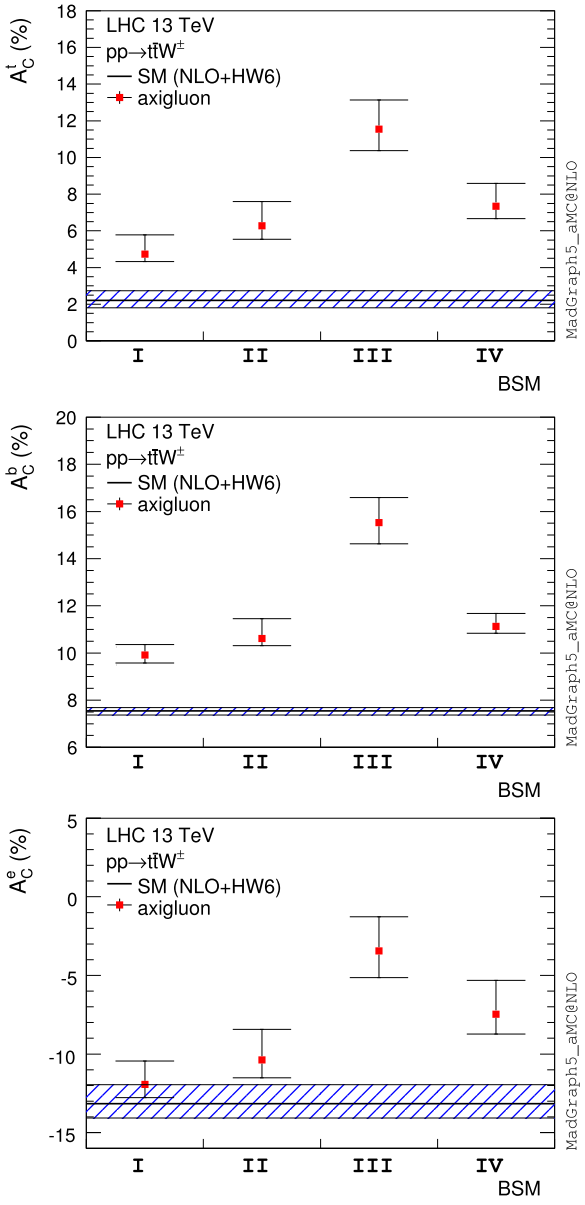

Fig. 7. Comparison between asymmetries predicted in the axigluon (NLO + BSM, I–IV) scenarios and the NLO SM prediction at 13 TeV, including scale uncertainties.

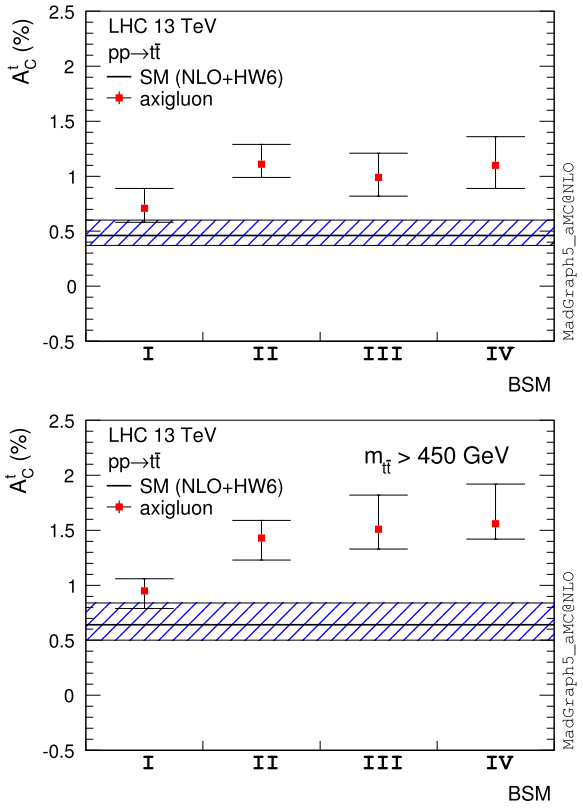

Fig. 8. Comparison between asymmetries predicted by axigluon (NLO + BSM, I–IV) scenarios and the NLO SM prediction at 13 TeV, for $t\bar{t}$ production, including scale uncertainties. Top panel: inclusive production. Bottom panel: $m_{t\bar{t}} > 450$ GeV.

The intrinsic QCD component of the asymmetry is nevertheless more stable, with A_c^t being reduced by at most 20% over the range 8–100 TeV. The values of $A_c^{b,\ell}$ obtained at 100 TeV by suppressing the spin correlations are $A_c^b = 1.47$ and $A_c^\ell = 1.55$, once again close to the value of $A_c^t = 1.85$.

The charge asymmetry in $t\bar{t}$ production, viceversa, is reduced by a factor ~ 6 when increasing the energy from 8 to 100 TeV. This is due to two effects related to the small-x behavior of the PDF's: first the gg channel, which is symmetric and therefore enters only in the denominator of Eq. (1) becomes more and more dominant; second the q and $\bar{q}$ asymmetry at large rapidities is less and less pronounced.

To derive a quantitative estimate of the statistical precision that could be optimistically reached under various energies and luminosity scenarios, we assume leptonic ($\ell = e, \mu$) decays for the top quarks

$$\sigma = \sigma\left(t\bar{t}W^{\pm}\right) \cdot \mathrm{BR}\left(t \to bl^{+}\nu_l\right)^2 = 0.0484 \cdot \sigma\left(t\bar{t}W^{\pm}\right),$$

and neglect acceptance and reconstruction efficiencies. Using the results collected in Table 6 we find:

Table 7
Contribution of the qg parton subprocess at NLO for the $t\bar{t}W^+$ process for $\mu_f = \mu_r = 2m_t$.

	8 TeV	13 TeV	14 TeV	33 TeV	100 TeV
$t\bar{t}W^+$ $(qg, \bar{q}g)$ (%)	7.5	15	17	33	51

Table 6
NLO + PS cross sections for $t\bar{t}$ and $t\bar{t}W^{\pm}$ and corresponding asymmetries at several cms energies. The quoted uncertainties are estimated with scale variations.

		8 TeV	13 TeV	14 TeV	33 TeV	100 TeV
$t\bar{t}$	σ (pb)	$198^{+15\%}_{-14\%}$	$661^{+15\%}_{-13\%}$	$786^{+14\%}_{-13\%}$	$4630^{+12\%}_{-11\%}$	$30700^{+13\%}_{-13\%}$
	A_c^t (%)	$0.72^{+0.14}_{-0.09}$	$0.45^{+0.09}_{-0.06}$	$0.43^{+0.08}_{-0.05}$	$0.26^{+0.04}_{-0.03}$	$0.12^{+0.03}_{-0.02}$
$t\bar{t}W^{\pm}$	σ (fb)	$210^{+11\%}_{-11\%}$	$587^{+13\%}_{-12\%}$	$678^{+14\%}_{-12\%}$	$3220^{+17\%}_{-13\%}$	$19000^{+20\%}_{-17\%}$
	A_c^t (%)	$2.37^{+0.56}_{-0.38}$	$2.24^{+0.43}_{-0.32}$	$2.23^{+0.43}_{-0.33}$	$1.95^{+0.28}_{-0.23}$	$1.85^{+0.21}_{-0.17}$
	A_c^b (%)	$8.50^{+0.15}_{-0.10}$	$7.54^{+0.19}_{-0.17}$	$7.50^{+0.24}_{-0.22}$	$5.37^{+0.22}_{-0.30}$	$3.36^{+0.15}_{-0.19}$
	A_c^e (%)	$-14.83^{-0.65}_{+0.95}$	$-13.16^{-0.81}_{+1.12}$	$-12.84^{-0.81}_{+1.11}$	$-9.21^{-0.87}_{+1.05}$	$-4.94^{-0.63}_{+0.72}$

- 8 TeV ($\mathcal{L} = 40$ fb^{-1}):

  $\delta_{\rm rel} A_c^t = 209\%, \quad \delta_{\rm rel} A_c^b = 58\%, \quad \delta_{\rm rel} A_c^\ell = 33\%,$

- 14 TeV ($\mathcal{L} = 300$ fb^{-1}):

  $\delta_{\rm rel} A_c^t = 45\%, \quad \delta_{\rm rel} A_c^b = 13\%, \quad \delta_{\rm rel} A_c^\ell = 8\%,$

- 14 TeV ($\mathcal{L} = 3000$ fb^{-1}):

  $\delta_{\rm rel} A_c^t = 14\%, \quad \delta_{\rm rel} A_c^b = 4\%, \quad \delta_{\rm rel} A_c^\ell = 2\%,$

- 100 TeV ($\mathcal{L} = 3000$ fb^{-1}):

  $\delta_{\rm rel} A_c^t = 3\%, \quad \delta_{\rm rel} A_c^b = 2\%, \quad \delta_{\rm rel} A_c^\ell = 1\%,$

where $\delta_{rel} A = \delta A / A$ is the relative precision on the asymmetries. While a realistic experimental analysis will certainly degrade this optimal precision, these numbers show the great potential of this observable.

We remark that the larger sensitivity of $A_c^{b,\ell}$ compared to A_c^t follows from the larger value of the former compared to the latter. The sensitivity to the purely QCD component of $A_c^{b,\ell}$, however, is comparable to the sensitivity of A_c^t. For example, at 100 TeV $\delta_{\rm rel} A_c^\ell = 1\%$ implies $\delta A_c^\ell \sim 0.0005$, which is about 3% of its QCD component, a precision consistent with what we quote for A_c^t.

In conclusion, the main motivation of our work has been the observation that the top quark charge asymmetry in $pp \to t\bar{t}W^\pm$ at the LHC is larger than that of inclusive $t\bar{t}$, being of a few percents. In addition, the lepton and b asymmetries are very large and already present at the leading order due to the polarization of the initial fermionic line by the $W^\pm$ emission. As a simple application, we have shown how the existence of an axigluon that could describe the Tevatron measurements of the forward–backward asymmetry would impact $pp \to t\bar{t}W^\pm$ and discussed the prospects in LHC Run II, HL-LHC and at future colliders.

The $t\bar{t}W^\pm$ final state will not replace the use of the $t\bar{t}$ asymmetry, particularly while the total integrated luminosity of the LHC is still below the O(100 fb^{-1}). In the long term, however, it will provide a powerful probe, complementary to the $t\bar{t}$ asymmetry, and uniquely sensitive to the chiral nature of possible new physics that were to manifest itself in these measurements.

Acknowledgements

We are thankful to Josh McFayden, Tamara Vazquez Schroeder and Elizaveta Shabalina for drawing our attention to features in $ttW^\pm$ MC simulations that inspired this investigation. We thank James Wells for useful remarks and discussions. This work has been supported in part by the ERC grant 291377 "LHC Theory", by the Research Executive Agency (REA) of the European Union under the Grant Agreement numbers PIT-GA-2010-264564 (LHCPhenoNet) and PITN-GA-2012-315877 (MCNet). The work of F.M. and I.T. is supported by the IISN "MadGraph" convention 4.4511.10, by the IISN "Fundamental interactions" convention 4.4517.08, and in part by the Belgian Federal Science Policy Office through the Interuniversity Attraction Pole P7/37. The work of M.Z. has been partly supported by the ILP LABEX (ANR-10-LABX-63), in turn supported by French state funds managed by the ANR within the "Investissements d'Avenir" programme under reference ANR-11-IDEX-0004-02.

Appendix A. $q_L\bar{q}_R \to t\bar{t}$ vs $q\bar{q} \to t\bar{t}W^\pm$

We first review the main features of polarized $q_L\bar{q}_R \to t\bar{t}$ scattering, on the same lines as $e_L^- e_R^+ \to t\bar{t}$ is discussed in Ref. [51].

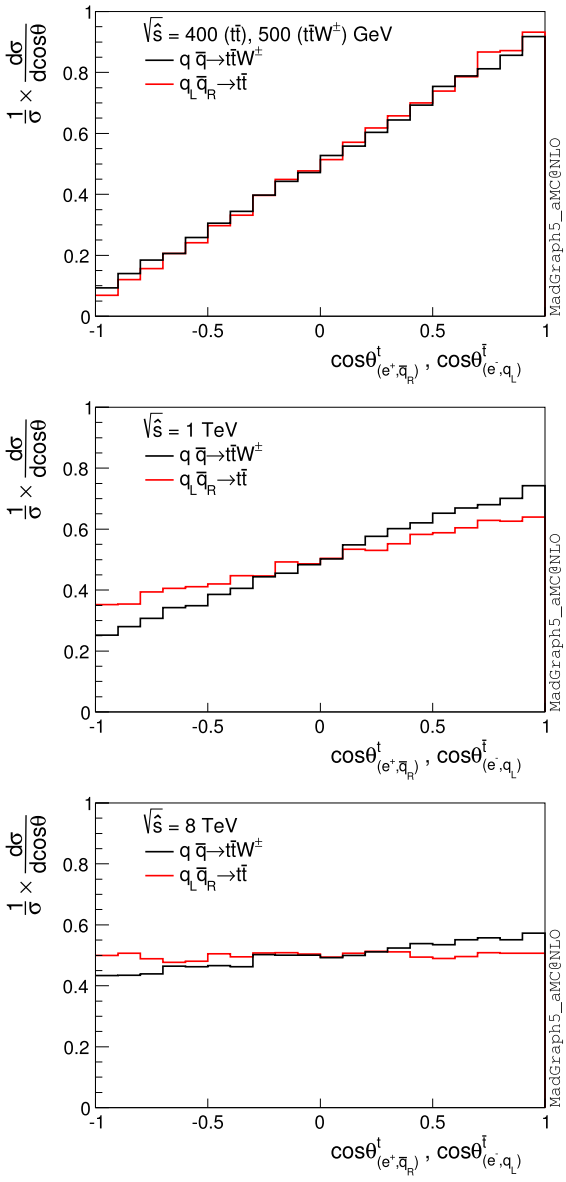

Fig. 9. Normalized $\cos\theta$ distributions for the leptons with respect to the spin axis for the $t, \bar{t}$ defined in the beam-axis as in Ref. [51] at different parton–parton energies (no PDF's). Close to threshold, *i.e.* 400 GeV for $t\bar{t}$ and 500 GeV for $t\bar{t}W^\pm$, the t and $\bar{t}$ are fully polarized. As the energy increases the distribution flattens out up to a constant at very high energies in agreement with Eq. (A.3).

In the beam line basis, *i.e.*, when the polarization axis of the top is the light antiquark direction in the top rest frame, the polarized differential cross sections $d\sigma_{t\text{pol},\bar{t}\text{pol}}$ for an initial state $q_L\ \bar{q}_R$ pair read

$$\begin{aligned}
\frac{d\sigma_{\uparrow\uparrow}}{d\cos\theta^*} &= \frac{d\sigma_{\downarrow\downarrow}}{d\cos\theta^*} = \mathcal{N}(\beta)\frac{\beta^2(1-\beta^2)\sin^2\theta^*}{(1+\beta\cos\theta^*)^2},\\
\frac{d\sigma_{\downarrow\uparrow}}{d\cos\theta^*} &= \mathcal{N}(\beta)\ \frac{\beta^4\sin^4\theta^*}{(1+\beta\cos\theta^*)^2},\\
\frac{d\sigma_{\uparrow\downarrow}}{d\cos\theta^*} &= \mathcal{N}(\beta)\frac{[(1+\beta\cos\theta^*)^2+(1-\beta^2)]^2}{(1+\beta\cos\theta^*)^2},
\end{aligned} \tag{A.1}$$

where $\mathcal{N}(\beta)$ is a normalization factor

$$\mathcal{N}(\beta) = \frac{\pi\alpha_S^2}{9s}\beta, \tag{A.2}$$

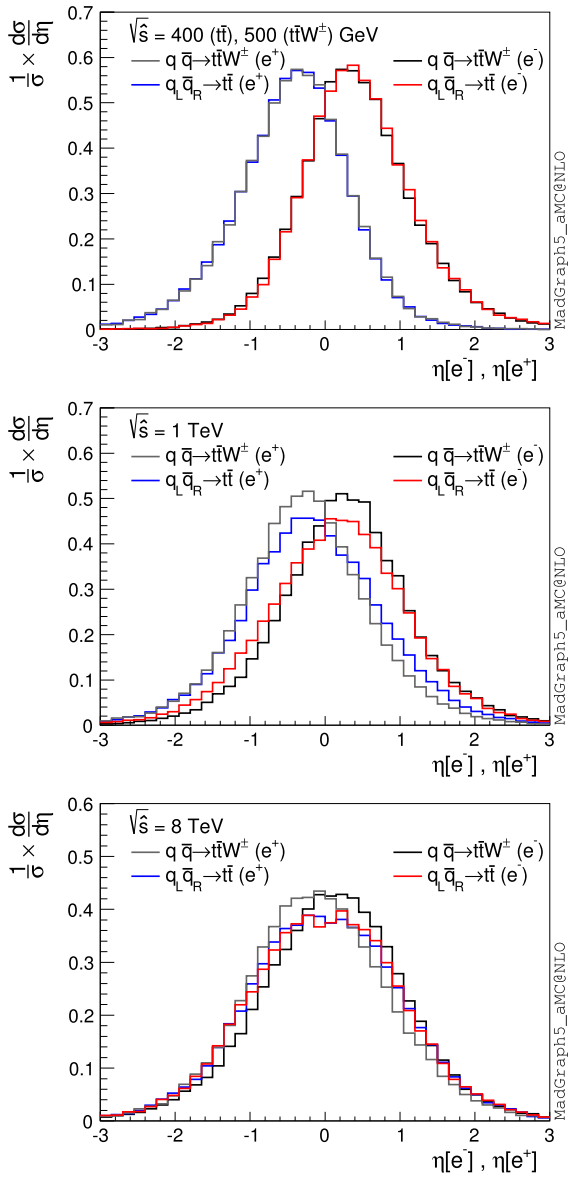

Fig. 10. Normalized pseudorapidity distributions in the $t\bar{t}$ center-of-mass frame. Close to threshold, *i.e.* 400 GeV for $t\bar{t}$ and 500 GeV for $t\bar{t}W^{\pm}$ full polarization of t and $\bar{t}$ determines a sizable opposite asymmetry in the distributions of the e^{+} and e^{-}. Far from threshold, the distribution becomes more and more symmetric.

and $\cos\theta^{*}$ is the polar angle of the top quarks in parton–parton center-of-mass frame. This basis is useful both at threshold ($\beta \to 0$), where it is clear that only one amplitude, $q_L\bar{q}_R \to t_{\uparrow}\bar{t}_{\downarrow}$ is non-zero, meaning that the top quarks are completely polarized, and at high energy ($\beta \to 1$), where it is manifest that the top anti-top polarizations are opposite,

$$\frac{d\sigma_{\uparrow\downarrow,\downarrow\uparrow}}{d\cos\theta^{*}} \overset{\beta\to 1}{=} \mathcal{N}(1)\left(1 \pm \cos\theta^{*}\right)^{2}, \tag{A.3}$$

a result which is also valid in the helicity basis [51]. Eq. (A.3) predicts the total number of events with opposite top anti-top polarization to be the same far from threshold. The polarization information is transferred to the decay products angular distributions, and in particular to the leptons that are 100% correlated with the top-quark spins.

One therefore expects the lepton polar distributions with respect to the beam axis to show a linear dependence in $\cos\theta_e$ at threshold that flattens out at high energies.

We have explicitly checked the expressions Eq. (A.1) and the analytic computation of the tree-level $q_L\bar{q}_R \to t\bar{t} \to b\ell^{+}\nu\bar{b}\ell^{-}\nu$ amplitude numerically to those obtained via MadGraph5_aMC@NLO. Apart from more complicated analytic formulas the case of $q\bar{q} \to t\bar{t}W^{\pm}$ is totally analogous, as the only non-trivial effect of the W-boson emission is that of selecting a $q_L\bar{q}_R$ in the initial state.

This is clearly shown in Figs. 9 and 10. In the first set of plots we show the lepton distributions from the top-quarks decay for both $q_L\bar{q}_R \to t\bar{t}$ and $q\bar{q} \to t\bar{t}W^{\pm}$ in the beam-axis frame at three values of $\sqrt{\hat{s}}$, one close to threshold (400 GeV for $t\bar{t}$ and 500 GeV for $t\bar{t}W^{\pm}$) and increasingly far from threshold (1 and 8 TeV). The two processes lead to very similar distributions. We have then considered the pseudorapidity distributions in the $t\bar{t}$ rest frame. We find that the t and the $\bar{t}$ pseudorapidity distributions are equal and symmetric at LO and we do not show them. The lepton distributions, however, see Fig. 10, display an opposite and equal forward–backward asymmetry whose shapes in the center-of-mass frame of the $t\bar{t}$ pair are again extremely similar in $q_L\bar{q}_R \to t\bar{t}$ and $q\bar{q} \to t\bar{t}W^{\pm}$. The fact that the asymmetry is larger at threshold is a direct consequence of the fact that there the top quarks are fully polarized.

References

[1] J.H. Kuhn, G. Rodrigo, Phys. Rev. Lett. 81 (1998) 49, arXiv:hep-ph/9802268.
[2] J.H. Kuhn, G. Rodrigo, Phys. Rev. D 59 (1999) 054017, arXiv:hep-ph/9807420.
[3] T. Aaltonen, et al., CDF Collaboration, Phys. Rev. D 87 (2013) 092002, arXiv:1211.1003 [hep-ex].
[4] T. Aaltonen, et al., CDF Collaboration, Phys. Rev. D 83 (2011) 112003, arXiv:1101.0034 [hep-ex].
[5] T.A. Aaltonen, et al., CDF Collaboration, arXiv:1404.3698 [hep-ex].
[6] V.M. Abazov, et al., D0 Collaboration, Phys. Rev. D 84 (2011) 112005, arXiv:1107.4995 [hep-ex].
[7] V.M. Abazov, et al., D0 Collaboration, arXiv:1405.0421 [hep-ex].
[8] M.T. Bowen, S.D. Ellis, D. Rainwater, Phys. Rev. D 73 (2006) 014008, arXiv:hep-ph/0509267.
[9] O. Antunano, J.H. Kuhn, G. Rodrigo, Phys. Rev. D 77 (2008) 014003, arXiv:0709.1652 [hep-ph].
[10] L.G. Almeida, G.F. Sterman, W. Vogelsang, Phys. Rev. D 78 (2008) 014008, arXiv:0805.1885 [hep-ph].
[11] W. Hollik, D. Pagani, Phys. Rev. D 84 (2011) 093003, arXiv:1107.2606 [hep-ph].
[12] A.V. Manohar, M. Trott, Phys. Lett. B 711 (2012) 313, arXiv:1201.3926 [hep-ph].
[13] W. Bernreuther, Z.-G. Si, Phys. Rev. D 86 (2012) 034026, arXiv:1205.6580 [hep-ph].
[14] J.A. Aguilar-Saavedra, D. Amidei, A. Juste, M. Perez-Victoria, arXiv:1406.1798 [hep-ph].
[15] G. Aad, et al., ATLAS Collaboration, J. High Energy Phys. 1402 (2014) 107, arXiv:1311.6724 [hep-ex].
[16] S. Chatrchyan, et al., CMS Collaboration, Phys. Lett. B 717 (2012) 129, arXiv:1207.0065 [hep-ex].
[17] CMS Collaboration, CMS-PAS-TOP-12-033.
[18] ATLAS Collaboration, ATLAS-CONF-2012-057.
[19] S. Chatrchyan, et al., CMS Collaboration, J. High Energy Phys. 1404 (2014) 191, arXiv:1402.3803 [hep-ex].
[20] ATLAS and CMS Collaborations, TOPLHC note, ATLAS-CONF-012, CMS PAS TOP-14-006.
[21] B. Ananthanarayan, J. Lahiri, M. Patra, S.D. Rindani, Phys. Rev. D 86 (2012) 114019, arXiv:1210.1385 [hep-ph].
[22] A. Brandenburg, M. Flesch, P. Uwer, Czechoslov. J. Phys. 50S1 (2000) 51, arXiv:hep-ph/9911249.
[23] S. Groote, J.G. Korner, B. Melic, S. Prelovsek, Phys. Rev. D 83 (2011) 054018, arXiv:1012.4600 [hep-ph].
[24] R. Harlander, M. Jezabek, J.H. Kuhn, T. Teubner, Phys. Lett. B 346 (1995) 137, arXiv:hep-ph/9411395.
[25] M. Cvetic, P. Langacker, Phys. Rev. D 46 (1992) 4943, arXiv:hep-ph/9207216; M. Cvetic, P. Langacker, Phys. Rev. D 48 (1993) 4484 (Erratum).
[26] R.J. Guth, J.H. Kuhn, Nucl. Phys. B 368 (1992) 38.
[27] M. Jezabek, J.H. Kuhn, Phys. Lett. B 329 (1994) 317, arXiv:hep-ph/9403366.
[28] V. Hirschi, R. Frederix, S. Frixione, M.V. Garzelli, F. Maltoni, R. Pittau, J. High Energy Phys. 1105 (2011) 044, arXiv:1103.0621 [hep-ph].
[29] J.M. Campbell, R.K. Ellis, J. High Energy Phys. 1207 (2012) 052, arXiv:1204.5678 [hep-ph].

[30] M.V. Garzelli, A. Kardos, C.G. Papadopoulos, Z. Trocsanyi, J. High Energy Phys. 1211 (2012) 056, arXiv:1208.2665 [hep-ph].
[31] A. Lazopoulos, K. Melnikov, F.J. Petriello, Phys. Rev. D 77 (2008) 034021, arXiv:0709.4044 [hep-ph].
[32] A. Lazopoulos, T. McElmurry, K. Melnikov, F. Petriello, Phys. Lett. B 666 (2008) 62, arXiv:0804.2220 [hep-ph].
[33] A. Kardos, Z. Trocsanyi, C. Papadopoulos, Phys. Rev. D 85 (2012) 054015, arXiv:1111.0610 [hep-ph].
[34] S. Badger, J.M. Campbell, R.K. Ellis, J. High Energy Phys. 1103 (2011) 027, arXiv:1011.6647 [hep-ph].
[35] J.A. Aguilar-Saavedra, E. Álvarez, A. Juste, F. Rubbo, J. High Energy Phys. 1404 (2014) 188, arXiv:1402.3598 [hep-ph].
[36] S. Chatrchyan, et al., CMS Collaboration, Phys. Rev. Lett. 110 (2013) 172002, arXiv:1303.3239 [hep-ex].
[37] A. Falkowski, M.L. Mangano, A. Martin, G. Perez, J. Winter, Phys. Rev. D 87 (2013) 034039, arXiv:1212.4003 [hep-ph].
[38] J. Alwall, R. Frederix, S. Frixione, V. Hirschi, F. Maltoni, O. Mattelaer, H.-S. Shao, T. Stelzer, et al., arXiv:1405.0301 [hep-ph].
[39] A.D. Martin, W.J. Stirling, R.S. Thorne, G. Watt, Eur. Phys. J. C 63 (2009) 189, arXiv:0901.0002 [hep-ph].
[40] P. Skands, B. Webber, J. Winter, J. High Energy Phys. 1207 (2012) 151, arXiv:1205.1466 [hep-ph].
[41] G. Corcella, I.G. Knowles, G. Marchesini, S. Moretti, K. Odagiri, P. Richardson, M.H. Seymour, B.R. Webber, J. High Energy Phys. 0101 (2001) 010, arXiv:hep-ph/0011363.
[42] S. Frixione, B.R. Webber, J. High Energy Phys. 0206 (2002) 029, arXiv:hep-ph/0204244.
[43] P. Artoisenet, R. Frederix, O. Mattelaer, R. Rietkerk, J. High Energy Phys. 1303 (2013) 015, arXiv:1212.3460 [hep-ph].
[44] M. Cacciari, G.P. Salam, G. Soyez, Eur. Phys. J. C 72 (2012) 1896, arXiv:1111.6097 [hep-ph].
[45] P. Ferrario, G. Rodrigo, Phys. Rev. D 80 (2009) 051701, arXiv:0906.5541 [hep-ph].
[46] P.H. Frampton, J. Shu, K. Wang, Phys. Lett. B 683 (2010) 294, arXiv:0911.2955 [hep-ph].
[47] A. Carmona, M. Chala, A. Falkowski, S. Khatibi, M.M. Najafabadi, G. Perez, J. Santiago, arXiv:1401.2443 [hep-ph].
[48] A. Alloul, N.D. Christensen, C. Degrande, C. Duhr, B. Fuks, arXiv:1310.1921 [hep-ph].
[49] S. Krastanov, http://feynrules.irmp.ucl.ac.be/wiki/topBSM.
[50] J. Alwall, C. Duhr, B. Fuks, O. Mattelaer, D.G. Ozturk, C.-H. Shen, arXiv:1402.1178 [hep-ph].
[51] S.J. Parke, Y. Shadmi, Phys. Lett. B 387 (1996) 199, arXiv:hep-ph/9606419.